

# Transcriptomics of a THEV-infected Turkey B-cell Line

Abraham Quaye<sup>†,a</sup>, Brian D. Poole<sup>a,\*</sup>

<sup>a</sup>Department of Microbiology and Molecular Biology, Brigham Young University

<sup>†</sup>First-author

<sup>\*</sup>Corresponding Author

## Corresponding Author Information

brian\_poole@byu.edu

Department of Microbiology and Molecular Biology,

4007 Life Sciences Building (LSB),

Brigham Young University,

Provo, Utah

<sup>14</sup> **ABSTRACT**

## INTRODUCTION

Turkey hemorrhagic enteritis virus (THEV), belonging to the family *Adenoviridae*, genus *Siadenovirus*, infects turkeys, chickens, and pheasants (1, 2). Infecting its hosts via the feco-oral route, THEV causes hemorrhagic enteritis (HE) in turkeys, a debilitating disease affecting predominantly 6-12 week old turkey poults characterized by immunosuppression (IMS), depression, splenomegaly, intestinal lesions leading to bloody droppings, and up to 80% mortality (3–6). The clinical disease usually persists in affected flocks for about 7-10 days. However, secondary bacterial infections may extend the duration of illness and mortality for an additional 2-3 weeks due to the immunosuppressive nature of the virus, exacerbating the economic losses (5, 7). Low pathogenic (avirulent) strains of THEV have been isolated, which show subclinical infections but retain the immunosuppressive effects. Since its isolation from a pheasant spleen, the Virginia Avirulent Strain (VAS) has been used effectively as a live vaccine despite the immunosuppressive side-effects but the vaccinated birds are rendered more susceptible to opportunistic infections and death than unvaccinated cohorts leading to significant economic losses (4, 5, 8–10).

It is well-established that THEV primarily infects and replicates in turkey B-cells of the bursa and spleen and somewhat in macrophages, inducing apoptosis and necrosis. Consequently, a significant drop in number of B-cells (specifically, IgM+ B-cells) and macrophages ensue along with increased T-cell counts with abnormal T-cell subpopulation (CD4+ and CD8+) ratios. The cell death seen in the B-cells and macrophages is generally proposed as the major cause of THEV-induced IMS as both humoral and cell-mediated immunity are impaired (5, 6, 8, 11). It is also thought that the virus replication in the spleen attracts T-cells and peripheral blood macrophages to the spleen where the T-cells are activated by cytokines from activated macrophages and vice versa. The activated T-cells undergo clonal expansion and secrete interferons: type I (IFN- $\alpha$  and IFN- $\beta$ ) and type II (IFN- $\gamma$ ) as well as tumor necrosis factor (TNF) while activated macrophages secrete interleukin 6 (IL-6), TNF, and nitric oxide (NO), an antiviral agent with immunosuppressive properties. The inflammatory cytokines released by T-cells and macrophages (e.g., TNF and IL-6) may also induce apoptosis in bystander splenocytes, exacerbating the already numerous apoptotic and necrotic splenocytes, culminating in IMS (8, 11) (see **Figure 1**). However, the precise molecular mechanisms of THEV-induced IMS or pathways involved are poorly understood (6). Elucidating the specific mechanisms and pathways of THEV-induced IMS is the most crucial step in THEV research as it will present a means of mitigating the IMS.

Next generation sequencing (NGS) is a groundbreaking technology that has significantly enhanced our understanding of DNA and RNA structure and function, and facilitated exceptional advancements in all domains of biology and the Life Sciences, including studies in rare genetic diseases, cancer genomics, microbiome analysis, infectious diseases, and population genetics (12). mRNA sequencing (RNA-seq), an

NGS approach to transcriptomic studies, is a versatile, high throughput, and cost-effective technology that allows a broad scan of the entire transcriptome (the complete set of RNA molecules produced under specific conditions or in specific cells), thereby uncovering the active genes and molecular pathways and processes. This technology has been leveraged in uncountable number of studies to elucidate active cellular processes under a wide range of treatment conditions, including the transcriptomics of viral infections (12–16). In RNA-seq studies, differentially expressed genes (DEGs) identified under different experimental conditions are key to unlocking the interesting biology or mechanism under study. Identified DEGs are typically used for functional enrichment analysis in large curated knowledgebases which connect genes to specific biological processes, functions, and pathways such as gene ontology (GO) and Kyoto Encyclopedia of Genes and Genomes (KEGG) pathways, shedding light on the biological question under study (17, 18).

To the best of our knowledge, no study has leveraged the wealth of information offered by RNA-seq to elucidate the molecular mechanisms and pathways leading to THEV-induced IMS. To effectively counteract the immunosuppressive effect of the vaccine, it is essential to unravel the host mechanisms/pathways influenced by the virus to bring about IMS. In this study, we present the first transcriptomic profile of a THEV infection using paired-end RNA-seq in a turkey B-cell line (MDTC-RP19), highlighting key host genes, cellular/molecular processes and pathways affected during a THEV infection. Our RNA-seq yielded 149 bp long high quality (mean PHRED Score of 36) sequences from each end of cDNA fragments, which were mapped to the genome of domestic turkey (*Meleagris gallopavo*).

## RESULTS

### Sequencing Results

To identify the host transcriptome profile of THEV infection, MDTC-RP19 cells were THEV-infected or mock-infected in triplicates or duplicates, respectively, and collected in like manner at 4-, 12-, 24-, and 72-hours post infection (hpi). mRNAs extracted from mock- or THEV-infected cells in duplicates or triplicates, respectively, were sequenced on the Illumina platform. The sequencing yielded a total of **776.1** million raw reads (149 bp in length) across all samples (statistics for the sequencing reads obtained from each RNA library are presented in **Table 1**). After trimming off low-quality reads, the remaining **742.8** million total paired-end trimmed reads (approximately, **34.7-47.9** million reads per sample) were mapped to the genome of *Meleagris gallopavo* obtained from the National Center for Biotechnology Information (NCBI). The percentage of reads mapping to the host genome across all samples ranged from **32.4-89.2%**. Although our sequencing reads have excellent quality scores (see **Table 1**) for all time points, the DEGs identified at 4- and 72-hpi did not yield any results in the functional enrichment analyses (i.e, GO term and KEGG pathway); hence, they were excluded from all subsequent analyses.

### DEGs of Infected Versus Mock-infected Cells

~~Discuss selection criteria and method/software used~~

~~Number of DEGs~~

~~Discuss all the QC plots (volcano, sample corr, pca, etc.) here~~

~~Discuss fold changes?~~

### Functional Enrichment Analyses (GO, KEGG pathway, and interaction network analyses)

~~Discuss enrichment analysis plots and tables here~~



## 87 CONCLUSIONS

## MATERIALS AND METHODS

### Cell culture and THEV Infection

The Turkey B-cell line (MDTC-RP19, ATCC CRL-8135) was grown as suspension cultures in 1:1 complete Leibovitz's L-15/McCoy's 5A medium with 10% fetal bovine serum (FBS), 20% chicken serum (ChS), 5% tryptose phosphate broth (TPB), and 1% antibiotic solution (100 U/mL Penicillin and 100 µg/mL Streptomycin), at 41°C in a humidified atmosphere with 5% CO<sub>2</sub>. Infected cells were maintained in 1:1 serum-reduced Leibovitz's L15/McCoy's 5A media (SRLM) with 2.5% FBS, 5% ChS, 1.2% TPB, and 1% antibiotic solution. A commercially available THEV vaccine was purchased from Hygieia Biological Labs (VAS strain). The stock virus was titrated using an in-house qPCR assay with titer expressed as genome copy number (GCN)/mL, similar to Mahshoub *et al* (19) with modifications. Cells were THEV-infected or mock-infected in triplicates or duplicates, respectively at a multiplicity of infection (MOI) of 100 GCN/cell, incubated at 41°C for 1 hour, and washed three times with phosphate buffered saline (PBS) to get rid of free virus particles. At each time point (4-, 12-, 24-, and 72-hpi), triplicate (THEV-infected) and duplicate (mock-infected) samples were harvested for total RNA extraction.

### RNA extraction and Sequencing

Total RNA was extracted from infected cells using the ThermoFisher RNAqueous™-4PCR Total RNA Isolation Kit (which includes a DNase I digestion step) per manufacturer's instructions. An agarose gel electrophoresis was performed to check RNA integrity. The RNA quantity and purity was initially assessed using nanodrop, and RNA was used only if the A260/A280 ratio was  $2.0 \pm 0.05$  and the A260/A230 ratio was  $>2$  and  $<2.2$ . Extracted total RNA samples were sent to LC Sciences, Houston TX for poly-A-tailed mRNA sequencing where RNA integrity was checked with Agilent Technologies 2100 Bioanalyzer High Sensitivity DNA Chip and poly(A) RNA-seq library was prepared following Illumina's TruSeq-stranded-mRNA sample preparation protocol. Paired-end sequencing, generating 150 bp reads was performed on the Illumina NovaSeq 6000 sequencing system. The paired-end 150bp sequences obtained during this study and all expression data have been submitted to the Gene Expression Omnibus database, under accession no #####

### Quality Control and Mapping Process

Sequencing reads were processed following a well-established protocol described by Pertea *et al* (20), using Snakemake - version 7.32.4 (21), a popular workflow management system to drive the pipeline. Briefly, raw sequencing reads were trimmed with Cutadapt - version 1.10 (22) and the quality of trimmed reads evaluated using the FastQC software, version 0.12.1 (Bioinformatics Group at the Babraham Institute, Cambridge, United Kingdom; [www.bioinformatics.babraham.ac.uk](http://www.bioinformatics.babraham.ac.uk)), achieving an overall Mean Sequence Quality (PHRED Score) of 36. Trimmed reads were mapped the reference *Meleagris gallopavo* genome



([https://ftp.ncbi.nlm.nih.gov/genomes/all/GCF/000/146/605/GCF\\_000146605.3\\_Turkey\\_5.1/GCF\\_000146605.3\\_Turkey\\_5.1\\_genomic.fna.gz](https://ftp.ncbi.nlm.nih.gov/genomes/all/GCF/000/146/605/GCF_000146605.3_Turkey_5.1/GCF_000146605.3_Turkey_5.1_genomic.fna.gz)) with Hisat2 - version 2.2.1 (20) using the accompanying gene transfer format (GTF) annotation file ([https://ftp.ncbi.nlm.nih.gov/genomes/all/GCF/000/146/605/GCF\\_000146605.3\\_Turkey\\_5.1/GCF\\_000146605.3\\_Turkey\\_5.1\\_genomic.gtf.gz](https://ftp.ncbi.nlm.nih.gov/genomes/all/GCF/000/146/605/GCF_000146605.3_Turkey_5.1/GCF_000146605.3_Turkey_5.1_genomic.gtf.gz)) to build a genomic index. Samtools - version 1.19.2 was used to convert the output Sequence Alignment Map (SAM) file to the more manageable Binary Alignment Map (BAM) format. The StringTie (v2.2.1) software (20), set to expression estimation mode was used to generate normalized gene expression estimates from the BAM files for genes in the reference GTF file after which the prepDE.py3 script was used to extract read count information from the StringTie gene expression files, providing an expression-count matrix for downstream DEG analysis.

### **DEG Analysis and Functional Enrichment Analysis**

DEG analysis between mock- and THEV-infected samples was performed using the very popular DESeq2 (23), which employs a Negative Binomial distribution model for read count comparisons. Genes with  $P_{\text{adjusted-value}} \leq 0.05$  were considered as differentially expressed. The read count data are deposited at Gene Expression Omnibus (GEO) under accession number ###. GO and KEGG analyses for DEGs were performed based on GO databases and KEGG databases using the R package gprofiler2 (24) with *Meleagris gallopavo* as the reference organism. Results with  $P_{\text{adjusted-value}} \leq 0.05$  were included as functionally enriched. Additionally, the DAVID analysis tool was used for KEGG pathway analysis. All visualization plots were made using ggplot2, pheatmap, and ggvenn R packages (25–27). Venn diagram —

### **Validation of DEGs by Reverse Transcriptase Quantitative PCR (RT-qPCR)**

### **Statistical Analysis**







## REFERENCES

1. Harrach B. 2008. Adenoviruses: General features, p. 1–9. *In* Mahy, BWJ, Van Regenmortel, MHV (eds.), Encyclopedia of virology (third edition). Book Section. Academic Press, Oxford.
2. Davison A, Benko M, Harrach B. 2003. Genetic content and evolution of adenoviruses. *The Journal of general virology* 84:2895–908.
3. Gross WB, Moore WE. 1967. Hemorrhagic enteritis of turkeys. *Avian Dis* 11:296–307.
4. Beach NM. 2006. Characterization of avirulent turkey hemorrhagic enteritis virus: A study of the molecular basis for variation in virulence and the occurrence of persistent infection. Thesis.
5. Dhama K, Gowthaman V, Karthik K, Tiwari R, Sachan S, Kumar MA, Palanivelu M, Malik YS, Singh RK, Munir M. 2017. Haemorrhagic enteritis of turkeys – current knowledge. *Veterinary Quarterly* 37:31–42.
6. Tykałowski B, Śmiałek M, Koncicki A, Ognik K, Zduńczyk Z, Jankowski J. 2019. The immune response of young turkeys to haemorrhagic enteritis virus infection at different levels and sources of methionine in the diet. *BMC Veterinary Research* 15.
7. Pierson F, Fitzgerald S. 2008. Hemorrhagic enteritis and related infections. *Diseases of Poultry* 276–286.
8. Rautenschlein S, Sharma JM. 2000. Immunopathogenesis of haemorrhagic enteritis virus (HEV) in turkeys. *Dev Comp Immunol* 24:237–46.
9. Larsen CT, Domermuth CH, Sponenberg DP, Gross WB. 1985. Colibacillosis of turkeys exacerbated by hemorrhagic enteritis virus. Laboratory studies. *Avian Dis* 29:729–32.

- 153 10. Beach NM, Duncan RB, Larsen CT, Meng XJ, Sriranganathan N, Pierson FW. 2009. Persistent infection of turkeys with an avirulent strain of turkey hemorrhagic enteritis virus. *Avian Diseases* 53:370–375.
- 154 11. Rautenschlein S, Suresh M, Sharma JM. 2000. Pathogenic avian adenovirus type II induces apoptosis in turkey spleen cells. *Archives of Virology* 145:1671–1683.
- 155 12. Satam H, Joshi K, Mangrolia U, Waghoo S, Zaidi G, Rawool S, Thakare RP, Banday S, Mishra AK, Das G, Malonia SK. 2023. Next-generation sequencing technology: Current trends and advancements. *Biology* 12:997.
- 156 13. Pandey D, Onkara Perumal P. 2023. A scoping review on deep learning for next-generation RNA-seq. Data analysis. *Functional & Integrative Genomics* 23.
- 157 14. Wang B, Kumar V, Olson A, Ware D. 2019. Reviving the transcriptome studies: An insight into the emergence of single-molecule transcriptome sequencing. *Frontiers in Genetics* 10.
- 158 15. Choi SC. 2016. On the study of microbial transcriptomes using second- and third-generation sequencing technologies. *Journal of Microbiology* 54:527–536.
- 159 16. Mo Q, Feng K, Dai S, Wu Q, Zhang Z, Ali A, Deng F, Wang H, Ning Y-J. 2023. Transcriptome profiling highlights regulated biological processes and type III interferon antiviral responses upon crimean-congo hemorrhagic fever virus infection. *Virologica Sinica* 38:34–46.
- 160 17. Ashburner M, Ball CA, Blake JA, Botstein D, Butler H, Cherry JM, Davis AP, Dolinski K, Dwight SS, Eppig JT, Harris MA, Hill DP, Issel-Tarver L, Kasarskis A, Lewis S, Matese JC, Richardson JE, Ringwald M, Rubin GM, Sherlock G. 2000. Gene ontology: Tool for the unification of biology. *Nature Genetics* 25:25–29.
- 161 18. Kanehisa M. 2000. KEGG: Kyoto encyclopedia of genes and genomes. *Nucleic Acids Research* 28:27–30.

- 162 19. Mahsoub HM, Evans NP, Beach NM, Yuan L, Zimmerman K, Pierson FW. 2017. Real-time PCR-based infectivity assay for the titration of turkey hemorrhagic enteritis virus, an adenovirus, in live vaccines. *Journal of Virological Methods* 239:42–49.
- 163 20. Pertea M, Kim D, Pertea GM, Leek JT, Salzberg SL. 2016. Transcript-level expression analysis of RNA-seq experiments with HISAT, StringTie and ballgown. *Nature Protocols* 11:1650–1667.
- 164 21. Mölder F, Jablonski KP, Letcher B, Hall MB, Tomkins-Tinch CH, Sochat V, Forster J, Lee S, Twardziok SO, Kanitz A, Wilm A, Holtgrewe M, Rahmann S, Nahnsen S, Köster J. 2021. Sustainable data analysis with snakemake. *F1000Research* 10:33.
- 165 22. Martin M. 2011. Cutadapt removes adapter sequences from high-throughput sequencing reads. *EMBnetjournal* 17:10.
- 166 23. Love MI, Huber W, Anders S. 2014. Moderated estimation of fold change and dispersion for RNA-seq data with DESeq2. *Genome Biology* 15:550.
- 167 24. Kolberg L, Raudvere U, Kuzmin I, Vilo J, Peterson H. 2020. gprofiler2— an r package for gene list functional enrichment analysis and namespace conversion toolset g:profiler. *F1000Research* 9 (ELIXIR).
- 168 25. Wickham H. 2016. ggplot2: Elegant graphics for data analysis. Springer-Verlag New York. <https://ggplot2.tidyverse.org>.
- 169 26. Kolde R. 2019. Pheatmap: Pretty heatmaps. <https://CRAN.R-project.org/package=pheatmap>.
- 170 27. Yan L. 2023. Ggvenn: Draw venn diagram by 'ggplot2'. <https://CRAN.R-project.org/package=ggvenn>.

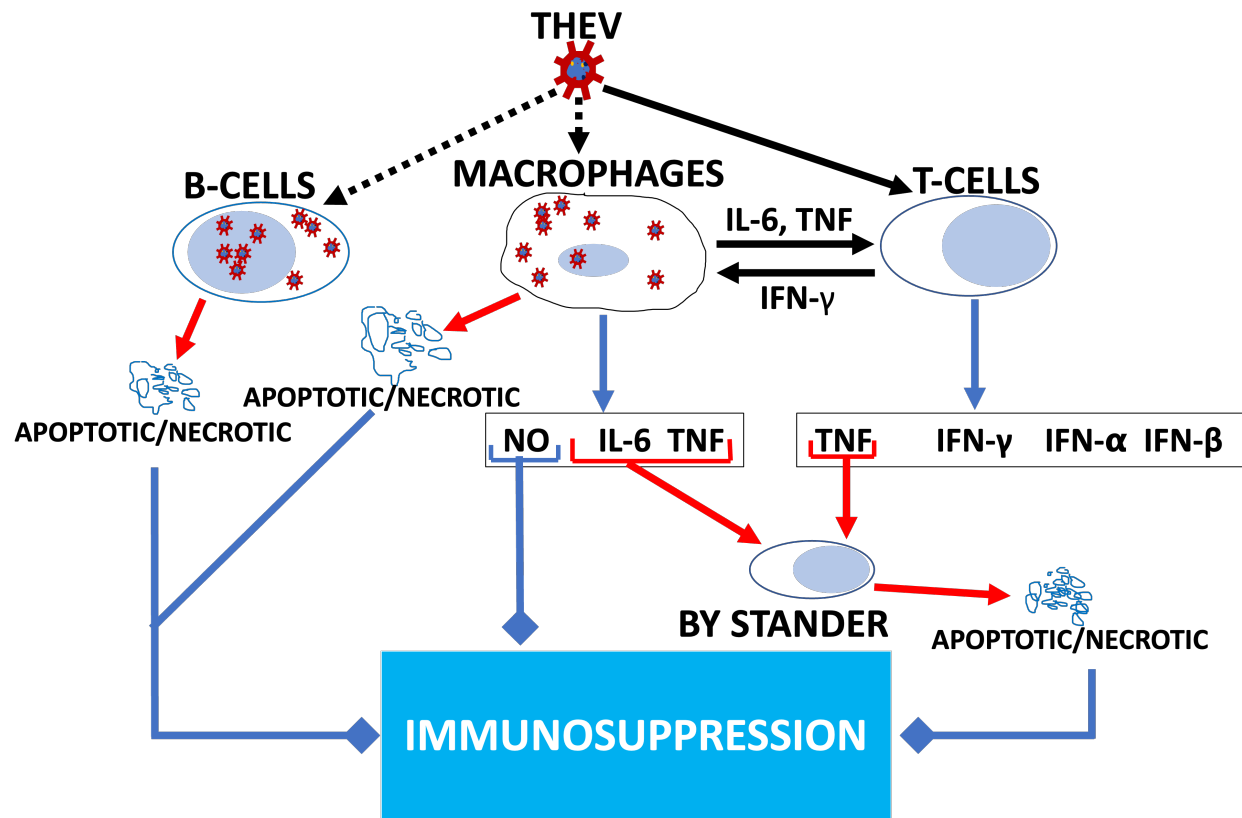


**Figure 1: Model of THEV-induced immunosuppression in turkeys.** THEV infection of target cells is indicated with black dotted arrows. Black unbroken arrows indicate cell activation. Red arrows indicated signals leading to apoptosis. Blue arrows indicate all cytokines released by the cell. Blue arrows with square heads indicated an event leading to IMS. Adapted from ((8))



Table 1: Summary of sequencing, quality control, and mapping processes

Sample	Raw Reads <sup>M</sup>	Trimmed Reads <sup>M</sup>	Mapped Reads <sup>M</sup>	Uniquely Mapped Reads <sup>M</sup>	Non-uniquely Mapped Reads <sup>M</sup>	Q20%	Q30%	GC Content (%)
I_12hrsS1 <sup>Inf</sup>	40.6	39.0	34.7 (88.92%)	33.1 (84.78%)	1.6 (4.14%)	99.95	97.23	47.5
I_12hrsS3 <sup>Inf</sup>	38.8	37.3	33.1 (88.78%)	31.7 (84.95%)	1.4 (3.83%)	99.95	97.53	47.5
I_24hrsS1 <sup>Inf</sup>	42.7	41.0	36.2 (88.13%)	34.5 (84.2%)	1.6 (3.93%)	99.95	96.95	46.5
I_24hrsS2 <sup>Inf</sup>	42.0	40.4	35.6 (88.1%)	33.9 (83.83%)	1.7 (4.27%)	99.94	97.05	46.5
I_24hrsS3 <sup>Inf</sup>	40.5	38.9	34.2 (88.01%)	32.7 (84.12%)	1.5 (3.89%)	99.95	97.08	47.0
I_4hrsS1 <sup>Inf</sup>	39.1	37.4	33 (88.16%)	31.2 (83.43%)	1.8 (4.73%)	99.93	97.04	48.5
I_4hrsS2 <sup>Inf</sup>	41.3	39.6	35.3 (89.24%)	33.6 (84.92%)	1.7 (4.33%)	99.95	97.15	47.0
I_4hrsS3 <sup>Inf</sup>	41.5	39.8	35.5 (89.2%)	33.2 (83.29%)	2.4 (5.91%)	99.95	97.11	47.5
I_72hrsS1 <sup>Inf</sup>	41.2	39.8	28.3 (71.09%)	26.9 (67.7%)	1.3 (3.38%)	99.96	97.23	44.5
I_72hrsS2 <sup>Inf</sup>	39.3	38.0	27 (71.11%)	25.8 (67.86%)	1.2 (3.25%)	99.96	97.34	44.5
I_72hrsS3 <sup>Inf</sup>	39.9	37.1	28.3 (76.36%)	26.1 (70.3%)	2.2 (6.05%)	99.87	96.14	52.5
U_12hrsN1 <sup>Mk</sup>	42.1	40.4	35.9 (88.72%)	34.1 (84.39%)	1.7 (4.33%)	99.95	97.04	47.5
U_12hrsN2 <sup>Mk</sup>	41.0	39.3	34.7 (88.4%)	33.2 (84.53%)	1.5 (3.86%)	99.94	97.08	47.5
U_24hrsN1 <sup>Mk</sup>	38.4	37.0	32.7 (88.46%)	31.4 (84.74%)	1.4 (3.72%)	99.96	97.48	47.5
U_24hrsN2 <sup>Mk</sup>	39.9	38.4	34 (88.58%)	32.6 (84.96%)	1.4 (3.61%)	99.95	96.95	47.0
U_4hrsN1 <sup>Mk</sup>	39.4	37.9	33.7 (88.9%)	32 (84.41%)	1.7 (4.49%)	99.96	97.36	47.0
U_4hrsN2 <sup>Mk</sup>	37.6	34.7	22 (63.43%)	18.5 (53.18%)	3.6 (10.25%)	99.80	94.96	61.0
U_72hrsN1 <sup>Mk</sup>	50.3	47.9	15.5 (32.4%)	11.7 (24.5%)	3.8 (7.9%)	99.88	96.54	56.0

Sample	Raw Reads <sup>M</sup>	Trimmed Reads <sup>M</sup>	Mapped Reads <sup>M</sup>	Uniquely Mapped Reads <sup>M</sup>	Non-uniquely Mapped Reads <sup>M</sup>	Q20%	Q30%	GC Content (%)
U_72hrsN2 <sup>Mk</sup>	40.5	38.9	34.5 (88.82%)	32.7 (84.14%)	1.8 (4.68%)	99.95	97.04	46.5

<sup>M</sup>All values for number of reads are in millions;

<sup>Inf</sup>These are infected samples indicated by the letter 'I' and 'S' in sample names

<sup>Mk</sup>These are mock-infected samples indicated by the letters 'U' and 'N' in sample names

